Supplement of Atmos. Chem. Phys., 21, 813–829, 2021
https://doi.org/10.5194/acp-21-813-2021-supplement

Atmospheric Chemistry and Physics
Open Access

Supplement of

Quantification of the role of stabilized Criegee intermediates in the formation of aerosols in limonene ozonolysis

Yiwei Gong and Zhongming Chen

Correspondence to: Zhongming Chen (zmchen@pku.edu.cn)

Chemicals used in this study

This study used the following: R-(+)-Limonene (Sigma-Aldrich, ≥ 99.0 %), 2-butanol (Sigma-Aldrich, ≥ 99.5 %), acetic acid (Sigma-Aldrich, ≥ 99.7%), ultrapure water (18MΩ, Millipore), N_2 (≥ 99.999 %, Beijing Haikeyuanchuang Practical Gas Company Limited, Beijing, China), O_2 (≥ 99.999 %, Beijing Haikeyuanchuang Practical Gas Company Limited, Beijing, China).

The wall loss fraction of SOA mass concentration

The wall loss fraction of SOA mass concentration is calculated as Eq. (S1):

$$F_{wall\ loss} = ([In] - [Out])/[In] \qquad (S1)$$

where $F_{wall\ loss}$ is the wall loss fraction of SOA mass concentration, [In] and [Out] are the SOA mass concentrations at the inlet and outlet of the reactor. Wall loss fractions at different relative humidity (RH) are shown in Table S1.

The formation and measurement of H_2O_2

When we estimated the yield of SCI_I in limonene ozonolysis, the formation of gas-phase H_2O_2 was measured, which was elaborated in our previous study (Gong et al., 2018). For the detection of gas-phase H_2O_2, the gas samples passing through the PTFE filter were collected in a glass coil collector at a temperature of 4 °C with H_3PO_4 solution (pH 3.5) serving as the rinsing solution. After the collection, solutions containing peroxides were analyzed by HPLC (Agilent 1100, USA) coupled with post-column derivatization and fluorescence detection online. Peroxides separated by column chromatography reacted with *p*-hydroxyphenylacetic acid (POPHA) to form POPHA dimers under the catalysis of hemin, and then the dimers were quantified using a fluorescence detector. With the increase of RH, it was observed that the yield of H_2O_2 increased significantly from dry conditions to 70% RH, and the H_2O_2 yield approached the limiting value above 70% RH, suggesting that reaction with water suppressed other reactions of SCI_I. In the exo-DB oxidation, the formation of hydroxymethyl hydroperoxide was also taken into consideration. Through the box model simulation, the contribution of HO_2 self-reaction to H_2O_2 formation was estimated to be limited. As for the reaction of SCIs with water, the products α-hydroxyalkyl hydroperoxides were reported to be preferential to decompose and generate H_2O_2 (Chen et al, 2016; Kumar et al, 2014). Although theoretical calculations indicated that the decomposition of α-hydroxyalkyl hydroperoxides was slow, some studies proved that water and acids could significantly catalyze the process (Anglada et al., 2002, 2011; Aplincourt and Anglada, 2003; Crehuet et al., 2001), and H_2O_2 formation occurred rapidly (Chen et al., 2016; Winterhalter et al., 2000). In addition, few α-hydroxyalkyl hydroperoxides larger than hydroxymethyl hydroperoxide were identified in gas phase, and the decomposition of α-hydroxyalkyl hydroperoxides was speculated to be totally completed.

The generation of H_2O_2 from aerosols in aqueous phase, which is mainly due to the decomposition of some compounds, has received attentions in recent years (Wang et al., 2011; Zhao et al., 2018). Here only the gas-phase H_2O_2 was detected to estimate the yield of SCI_I, while it was still needed to analyze whether the formation of H_2O_2 in SOA could impact the results. Zhao et al. (2018) reported the aqueous decomposition rate coefficients of α-acyloxyalkyl hydroperoxides, whose lifetime was estimated to be about 24 min in liquid aerosols. As the reaction time in flow tube reactors was around 4 min, the H_2O_2 formation from aerosols was not considered to contribute much to gas-phase H_2O_2. In addition, it was found that the dependence of H_2O_2 yield on RH could be well simulated with the gas-phase mechanisms, confirming that the particle-phase formation of H_2O_2 did not make obvious impact on the results.

Calculating the amount of SCIs consumed by water

Here the amount of SCIs consumed by water could not be derived directly, and it was calculated through the reaction rate ratio of SCIs reaction with water and AA as Eqs. (S2) and (S3):

$$\frac{SCI_{H2O}}{SCI_{AA}} = \frac{k_{(SCI+H2O)\mathrm{I}} \cdot [H_2O] \cdot SCI_{\mathrm{I}}}{k_{(SCI+AA)} \cdot [AA] \cdot SCI_{Total}} \qquad (S2)$$

$$SCI_{H2O} = \frac{k_{(SCI+H2O)\mathrm{I}} \cdot [H_2O] \cdot 0.545}{k_{(SCI+AA)} \cdot [AA]} \cdot \Delta AA \qquad (S3)$$

where SCI_{H2O} (molecule cm^{-3}) is the amount of SCIs reacted with H_2O; SCI_{AA} (molecule cm^{-3}) is the amount of SCIs reacted with AA; $k_{(SCI+H2O)I}$ (cm^3 molecule^{-1} s^{-1}) is the rate constant of SCI_I reaction with H_2O; $k_{(SCI+AA)}$ (cm^3 molecule^{-1} s^{-1}) is the rate constant of SCIs reaction with AA; $[H_2O]$ (molecule cm^{-3}) is the concentration of H_2O; [AA] (molecule cm^{-3}) is the concentration of AA; SCI_I (molecule cm^{-3}) is the amount of SCI_I generated; SCI_{Total} (molecule cm^{-3}) is the amount of total SCIs generated; ΔAA (molecule cm^{-3}) is the amount of AA consumed.

SCI_I reaction with H_2O and $(H_2O)_2$

To acquire the reaction rate ratio of SCIs reaction with water and AA, it should be figured out whether the reaction with H_2O or $(H_2O)_2$ dominants in SCI_I reaction with water. This problem was discussed by estimating the generation of H_2O_2, which is a major product formed from SCI_I reaction with water (Hasson et al., 2001; Winterhalter et al., 2000). The dependence of H_2O_2 yield on RH reported in our previous study is shown in Fig. S2 (Gong et al., 2018), we estimated the formation of H_2O_2 based on SCI_I reaction with H_2O and SCI_I reaction with $(H_2O)_2$, respectively. The inferred relationships between H_2O_2 and the concentrations of H_2O and $(H_2O)_2$ are shown as Eqs. (S4)–(S7):

$$\frac{SCI_{H2O}}{SCI_{\mathrm{I}}} = \frac{\Delta H_2O_2}{SCI_{\mathrm{I}}} = \frac{k_{(SCI+H2O)\mathrm{I}} \cdot [H_2O]}{k_{(SCI+H2O)\mathrm{I}} \cdot [H_2O] + k_{(other)\mathrm{I}}} \tag{S4}$$

$$\Delta H_2O_2 = \frac{1}{1 + \frac{k_{(other)\mathrm{I}}}{k_{(SCI+H2O)\mathrm{I}} \cdot [H_2O]}} \cdot SCI_{\mathrm{I}} \tag{S5}$$

$$\frac{SCI_{(H2O)2}}{SCI_{\mathrm{I}}} = \frac{\Delta H_2O_2}{SCI_{\mathrm{I}}} = \frac{k_{(SCI+(H2O)2)\mathrm{I}} \cdot [(H_2O)_2]}{k_{(SCI+(H2O)2)\mathrm{I}} \cdot [(H_2O)_2] + k_{(other)\mathrm{I}}} \tag{S6}$$

$$\Delta H_2O_2 = \frac{1}{1 + \frac{k_{(other)\mathrm{I}}}{k_{(SCI+(H2O)2)\mathrm{I}} \cdot [(H_2O)_2]}} \cdot SCIs_{\mathrm{I}} \tag{S7}$$

where SCI_{H2O} (molecule cm^{-3}) is the amount of SCIs reacted with H_2O; SCI_I (molecule cm^{-3}) is the amount of SCI_I generated; ΔH_2O_2 (molecule cm^{-3}) is the amount of H_2O_2 generated; $[H_2O]$ (molecule cm^{-3}) is the concentration of H_2O; $[(H_2O)_2]$ (molecule cm^{-3}) is the concentration of $(H_2O)_2$; $k_{(SCI+H2O)I}$ (cm^3 molecule^{-1} s^{-1}) is the rate constant of SCI_I reaction with H_2O; $k_{(SCI+(H2O)2)I}$ (cm^3 molecule^{-1} s^{-1}) is the rate constant of SCI_I reaction with $(H_2O)_2$; $k_{(other)I} = k_{(isomerization)I} + k_{(SCI+products)I} \cdot [products]$, meaning that $k_{(other)I}$ accounts for the sum of SCI_I isomerization and reaction with other products in the system. In Fig. S2, the red line represents the estimated yield of H_2O_2 based on SCI_I reaction with H_2O when $k_{(SCI+H2O)I}$ is set as 5×10^{-16} cm^3 molecule^{-1} s^{-1} and $k_{(other)I}$ is 30 s^{-1}; the green line represents the estimated yield of H_2O_2 based on SCI_I reaction with $(H_2O)_2$ when $k_{(SCI+(H2O)2)I}$ is set as 1×10^{-12} cm^3 molecule^{-1} s^{-1} and $k_{(other)I}$ is 30 s^{-1}. The estimation based on SCI_I reaction with H_2O showed a better fitting with the measured results and $k_{(SCI+H2O)I}$ was used to calculate the amount of SCIs reacted with water.

Calculating the amount of exocyclic double bonds (exo-DB) ozonated in bulk phase

Here the second-generation oxidation at 80% RH was analyzed. Results showed that at 80% RH the amount of exo-DB ozonated was ~ 15 ppbv larger than that under dry condition. Assuming that particles at 80% RH were liquid and exo-DB were ozonated in bulk phase, the amount of exo-DB ozonated in bulk phase could be calculated according to Eq. (S8):

$$\Delta\left[DB_{(aq)}\right] = k_{(aq)} \cdot \left[{O_3}_{(aq)}\right] \cdot \left[DB_{(aq)}\right] \cdot t \qquad (S8)$$

where $\Delta[DB_{(aq)}]$ ($mol\ L^{-1}$) is the amount of exo-DB ozonated in bulk phase; $k_{(aq)}$ ($L\ mol^{-1}\ s^{-1}$) is the rate constant of exo-DB ozonated in bulk phase; $[O_{3(aq)}]$ ($mol\ L^{-1}$) is the concentration of O_3 in bulk phase; $[DB_{(aq)}]$ ($mol\ L^{-1}$) is the concentration of exo-DB in bulk phase; t (s) is the reaction time. During the reaction, although bulk-phase exo-DB and O_3 were consumed, gas-phase O_3 and SVOCs containing exo-DB would constantly enter bulk phase, and it was hypothesized that both of $[O_{3(aq)}]$ and $[DB_{(aq)}]$ could maintain stable during reaction. Based on measurement results, the average SOA mass concentration in the second-generation oxidation was around 50 μg m^{-3}, and $\Delta[DB_{(aq)}]$ was derived to be 15.94 mol L^{-1}. $[O_{3(aq)}]$ was calculated through Henry's law as Eq. (S9):

$$H_{O3} = \frac{\left[{O_3}_{(aq)}\right]}{P_{O3}} \qquad (S9)$$

where H_{O3} ($mol\ L^{-1}\ Pa^{-1}$) is the Henry's law constant of O_3, which is 9.28×10^{-8} mol L^{-1} Pa^{-1} at 298 K (Sander, 2015); P_{O3} (Pa) is the partial pressure of O_3 in the gas phase. It was calculated that $[O_{3(aq)}]$ was 1.10×10^{-7} mol L^{-1}, and the rate constant of unsaturated first-generation oxidation products ozonated in aqueous phase was reported to be about 4.0×10^{4} L mol^{-1} s^{-1}(Witkowski et al., 2018a, b), according to which $[DB_{(aq)}]$ was derived to be 15.09 mol L^{-1}. Assuming that the molecular weight of unsaturated first-generation products was 200 g mol^{-1}, the density of those particulate unsaturated compounds was 3.02 g cm^{-3}, which was even larger than the aerosol density of 1.30 g cm^{-3}, suggesting that bulk-phase ozonolysis was not able to explain the large amount of exo-DB ozonated under high-humidity conditions.

Estimating the uptake coefficient of unsaturated first-generation products on aqueous aerosols

Here the second-generation oxidation at 80% RH was analyzed. The uptake coefficient of unsaturated first-generation products can be estimated when simplifying the heterogeneous reaction as a pseudo-first-order reaction using Eq. (S10) (Ravishankara, 1997):

$$\gamma = \frac{4k}{\omega A} \qquad (S10)$$

where γ is the uptake coefficient of unsaturated products; k (s^{-1}) is the rate constant of pseudo-first-order reaction; ω ($m\ s^{-1}$) is the mean molecular velocity; A ($m^2\ m^{-3}$) is the total surface area concentration of particles. ω is calculated using Eq. (S11):

$$\omega = \sqrt{\frac{8RT}{\pi M_x}} \qquad (S11)$$

where R ($J\ mol^{-1}\ K^{-1}$) is the gas constant; T (K) is the absolute temperature; M_x ($kg\ mol^{-1}$) is the molar weight of unsaturated first-generation products, which is assumed to be 0.2 $kg\ mol^{-1}$ and ω is derived as 178 $m\ s^{-1}$. During the second-generation oxidation the amount of exo-DB ozonated through heterogeneous reaction at 80% RH was around 15 ppbv, and since the heterogeneous reaction process here was treated as a pseudo-first-order reaction, k could be calculated through Eq. (S12):

$$\Delta[DB] = k \cdot [O_3] \cdot t \qquad (S12)$$

where Δ[DB] ($molecule\ cm^{-3}$) is the amount of exo-DB ozonated through heterogeneous reaction; $[O_3]$ ($molecule\ cm^{-3}$) is the concentration of O_3; t (s) is the reaction time. O_3 concentration in the second-generation oxidation was 11.9 ppmv and the reaction time was 240 s, so k was calculated to be $5.25 \times 10^{-6}\ s^{-1}$. The surface area concentration of aerosols in the second-generation oxidation was estimated to be $\sim 4 \times 10^{-5}\ m^2\ m^{-3}$, and γ was derived to be 2.95×10^{-3}.

SOA formation in the first-generation oxidation

Growth curves of SOA mass concentration and SOA yield in the first-generation oxidation are shown in Fig. S4. It is noted that the SOA growth curve at certain RH is similar to the curve at the adjacent RH, and for instance, SOA growth curves of 10% and 20% RH are similar with each other. The same situation is observed between conditions of 30% and 40% RH, and SOA growth above 60% RH seems unchanged with RH increasing. To better identify SOA growth curves at different RH in the picture, conditions of < 0.5%, 10%, 30%, 50%, 70%, and 90% RH are chosen to show.

Estimating the amount of SCIs scavenged by excess AA

When adding excess AA (10.0 ± 0.4 ppmv) into the reaction system, the amount of SCIs consumed by AA could be estimated as Eq. (S13):

$$\frac{SCI_{AA}}{SCI} = \frac{k_{(SCI+AA)} \cdot [AA]}{k_{(SCI+H2O)} \cdot [H_2O] + k_{(other)}} \qquad (S13)$$

where SCI_{AA} (molecule cm^{-3}) is the amount of SCIs reacted with AA; SCI (molecule cm^{-3}) is the amount of SCI generated; [AA] (molecule cm^{-3}) is the concentration of AA; [H_2O] (molecule cm^{-3}) is the concentration of H_2O; $k_{(SCI+AA)}$ (cm^3 molecule^{-1} s^{-1}) is the rate constant of SCI reaction with AA; $k_{(SCI+H2O)}$ (cm^3 molecule^{-1} s^{-1}) is the rate constant of SCI reaction with H_2O; $k_{(other)}$ = $k_{(isomerization)I}$ + $k_{(SCI+products)}$ · [products], meaning that $k_{(other)}$ accounts for the sum of SCI isomerization and reaction with other products in the system. Using the parameters derived in the study, reactions of SCI_I and SCI_{II} were both considered and it was calculated that even under 90% RH the concentration of AA used was sufficient for scavenging more than 99% of SCIs generated during reactions.

The fraction of SCIs converting into SOA (α_{SCI})

The slope of the fitting line of SOA versus SCIs represents the amount of SOA contributed by per unit concentration of SCIs, which is denoted as SOA_{perSCI}. When taking the average of the slopes in the first- and second-generation oxidations, SOA_{perSCI} under dry and low-humidity conditions was calculated to be 1.39 μg m^{-3}, and under high-humidity conditions SOA_{perSCI} was 2.46 μg m^{-3}. In theory, if all SCIs could convert into SOA by producing low-volatile products, of which the molar mass was assumed to be 200 g mol^{-1}, it was estimated that SOA_{perSCI} was 8.17 μg m^{-3}. As the molar mass of products formed from monoterpene-derived SCIs was expected to be large (Lee and Kamens, 2005), SOA_{perSCI} was calculated to be 12.26 μg m^{-3} when assuming the molar mass of the products was 300 g mol^{-1}. It was derived that under dry and low-humidity conditions α_{SCI} was 11–17% and under high-humidity conditions α_{SCI} was 20–30%.

The amount of SOA formed from SCIs reaction could be estimated as Eqs. (S14) and (S15) when assuming the molar weight of low-volatile products formed from SCIs is 300 g mol^{-1}:

$$SOA_{SCI} = \alpha_{SCI} \cdot SCI \cdot \frac{1}{N_A} \cdot 3 \times 10^{14} \qquad (S14)$$

$$SOA_{SCI} = 5 \times 10^{-10} \alpha_{SCI} \cdot SCI \qquad (S15)$$

where SOA_{SCI} (μg m^{-3}) is the mass concentration of SOA formed from SCIs reaction; SCI (molecule cm^{-3}) is the amount of SCIs in reaction system; α_{SCI} is the conversion rate of SCIs that are valid for SOA formation; N_A (6.02 × 10^{23} molecule mol^{-1}) is the Avogadro constant. When water exists, SCI at different RH could be calculated as Eqs. (S16) and (S17):

$$SCI = SCI_{Total} - \frac{1}{1 + \frac{k_{(other)\mathrm{I}}}{k_{(SCIs+H2O)\mathrm{I}} \cdot [H_2O]}} \cdot SCI_{\mathrm{I}} \qquad (S16)$$

$$SCI = SCI_{Total} - \frac{RH}{RH + 7.8} \cdot SCI_{\mathrm{I}} \qquad (S17)$$

where RH (%) is the relative humidity.

Experiments with cyclohexane as OH scavenger

Part of SCIs might react with 2-butanol, producing α-alkoxyalkyl-hydroperoxides and contributing to the observed SOA, especially when using low concentrations of AA and water. To figure out whether the SOA formation potentials of SCIs estimated here were higher than those under the situation without 2-butanol, the experiments with cyclohexane as OH scavenger were carried out. Here three representative conditions: dry conditions, 40% RH (representing low-humidity conditions) and 80% RH (representing high-humidity conditions), were analyzed in the endo-DB ozonolysis. The abilities of 2-butanol and cyclohexane on scavenging OH radicals were similar (Chew and Atkinson, 1996), however, the use of different OH scavengers brought different impacts on the reaction system. When 2-butanol was used, higher $[HO_2]/[RO_2]$ was observed, which was thought to be more similar to the atmospheric conditions, while adding cyclohexane resulted in a lower $[HO_2]/[RO_2]$ (Docherty and Ziemann, 2003; Jonsson et al., 2008). In view of this, this study chose 2-butanol as OH scavenger, while the use of cyclohexane could provide a contrast to help us better understand the mechanisms in the reaction system.

In the experiments with cyclohexane, the concentrations of limonene and O_3 were about 90 ppbv and 270 ppbv, and the reaction time was 240 s. Around 400 ppmv of cyclohexane was added to scavenge OH radicals. With the addition of cyclohexane, the SOA yields were found to be lower than those with the addition of 2-butanol, suggesting that higher concentration of HO_2 radicals promoted aerosols formation (Keywood et al., 2004). Through adding different concentrations of AA (24–480 ppbv), the amount of SCIs in the reaction system was regulated and calculated as elaborated in Sect. 3.1, and the dependence of SOA mass concentration on the amount of SCIs was shown in Fig. S8. The SCIs reactions still accounted for more than 60% in SOA formation and according to the fitting results, the SOA formation potentials of SCIs under the use of cyclohexane were even a bit larger than those under the use of 2-butanol, and the deviations were within 12%. This phenomenon was speculated to be due to the higher concentration of RO_2 radicals when using cyclohexane, promoting the reactions of SCIs with RO_2.

The effect of the concentrations of reactants on the results

In this study, to get enough products for analysis in a short reaction time, both of the concentrations of limonene and O_3 used in experiments were higher than those in the real atmosphere, and it was needed to consider the effect of concentrations of reactants. In the atmosphere, the concentrations of organic compounds formed from limonene ozonolysis are much smaller than those in flow tube reactors, while it should be noted that limonene-derived SCIs would not only react with the compounds formed from limonene, they could also react with other compounds in the ambient air. In this study, we determined the rate of SCIs isomerization and reaction with other products. In the atmosphere, the organic compounds that SCIs could react with are generally carboxylic acids, carbonyls, alcohols, and RO_2 radicals, and the concentrations of these compounds in forest are about 10^{11} molecule cm^{-3}, 10^{11} molecule cm^{-3}, 10^{11} molecule cm^{-3}, and 10^{9} molecule cm^{-3}, respectively. In urban area, the concentrations of carbonyls and alcohols were reported to be higher because of the anthropogenic emissions (Vereecken et al., 2012). The rate coefficients of SCIs reaction with carboxylic acids, carbonyls, alcohols, and RO_2 radicals were reported to be around 10^{-10} molecule cm^{3} s^{-1}, 10^{-12} molecule cm^{3} s^{-1}, 10^{-14} molecule cm^{3} s^{-1}, and 10^{-11} molecule cm^{3} s^{-1}, respectively

(Khan et al., 2018; Lin and Chao, 2017; Zhao et al., 2017). It was estimated that the sum of the rate of SCIs isomerization and reaction with organic compounds in the atmosphere was on the same order of magnitude as that in experiments, and thus the results obtained here were considered to be feasible to the ambient conditions. We declare that further studies on different concentrations of reactants with the coexistence of other organic compounds would make the results more concise.

Figure caption

Table S1. Wall loss fractions of SOA mass concentration at different relative humidity (RH).

Table S2. The amounts of SCIs (molecule cm^{-3}) under different concentrations of acetic acid (AA, molecule cm^{-3}) and different relative humidity (RH) in the first-generation oxidation.

Table S3. The amounts of SCIs (molecule cm^{-3}) under different concentrations of acetic acid (AA, molecule cm^{-3}) and different relative humidity (RH) in the second-generation oxidation.

Table S4. The reactants concentrations (ppbv) in calculations of steady-state concentrations of SCIs in forest, urban area, and indoor area.

Figure S1. Diagram of the thermostatic coil collector.

Figure S2. The dependence of the molar yield of hydrogen peroxide (H_2O_2) on relative humidity (RH).

Figure S3. The variation of the consumption of acetic acid (ΔAA) with the concentration of acetic acid ([AA]) at different relative humidity (RH) in the second-generation oxidation.

Figure S4. Growth curves of (a) SOA mass concentration (SOA) and (b) SOA yield (Y) versus limonene reacted (△HC) at different relative humidity (RH) in the first-generation oxidation.

Figure S5. Growth curves of (a) SOA mass concentration (SOA) and (b) SOA yield (Y) versus reaction time at different relative humidity (RH) in the second-generation oxidation.

Figure S6. The variation of SOA mass concentration (SOA) with the concentration of acetic acid ([AA]) at different relative humidity (RH) in the second-generation oxidation.

Figure S7. Structures of limonene-derived SCIs formed from endo-DB and exo-DB ozonolysis.

Figure S8. The dependence of SOA mass concentration on the amount of SCIs at different relative humidity (RH) in the first-generation oxidation with cyclohexane as OH scavenger.

References

Anglada, J. M., Aplincourt, P., Bofill, J. M., and Cremer, D.: Atmospheric formation of OH radicals and H_2O_2 from alkene ozonolysis under humid conditions, Chem. Phys. Chem., 3, 215–221, doi: 10.1002/1439-7641(20020215)3:2<215::Aid-Cphc215>3.3.Co;2-V, 2002.

Anglada, J. M., González, J., and Torrent-Sucarrat, M.: Effects of the substituents on the reactivity of carbonyl oxides. A theoretical study on the reaction of substituted carbonyl oxides with water, Phys. Chem. Chem. Phys., 13, 13034–13045, doi: 10.1039/C1CP20872A, 2011.

Aplincourt, P. and Anglada, J. M.: Theoretical studies of the isoprene ozonolysis under tropospheric conditions. 2. Unimolecular and water-assisted decomposition of the α-hydroxy hydroperoxides, J. Phys. Chem. A, 107, 5812–5820, doi: 10.1021/jp034203w, 2003.

Boy, M., Mogensen, D., Smolander, S., Zhou, L., Nieminen, T., Paasonen, P., Plass-Dülmer, C., Sipilä, M., Petäjä, T., Mauldin, L., Berresheim, H., and Kulmala, M.: Oxidation of SO_2 by stabilized Criegee intermediate (sCI) radicals as a crucial source for atmospheric sulfuric acid concentrations, Atmos. Chem. Phys., 13, 3865–3879, doi: 10.5194/acp-13-3865-2013, 2013.

Carslaw, N.: A new detailed chemical model for indoor air pollution, Atmos. Environ., 41, 1164–1179, doi: 10.1016/j.atmosenv.2006.09.038, 2007.

Chen, L., Wang, W. L., Wang, W. N., Liu, Y. L., Liu, F. Y., Liu, N., and Wang, B. Z.: Water-catalyzed decomposition of the simplest Criegee intermediate CH_2OO, Theor. Chem. Acc., 135, 131, doi: 10.1007/s00214-016-1894-9, 2016.

Chew, A. A. and Atkinson, R.: OH radical formation yields from the gas-phase reactions of O_3 with alkenes and monoterpenes, J. Geophys. Res., 101, 28649–28653, doi: 10.1029/96JD02722, 1996.

Crehuet, R., Anglada, J. M., and Bofill, J. M.: Tropospheric formation of hydroxymethyl hydroperoxide, formic acid, H_2O_2, and OH from carbonyl oxide in the presence of water vapor: A theoretical study of the reaction mechanism, Chem. Eur. J., 7, 2227–2235, doi: 10.1002/1521-3765(20010518)7:10<2227::AID-CHEM2227>3.0.CO;2-O, 2001.

Docherty, K. S. and Ziemann, P. J.: Effects of stabilized Criegee intermediate and OH radical scavengers on aerosol formation from reactions of β-pinene with O_3, Aerosol Sci. Technol., 37, 877–891, doi: 10.1080/02786820300930, 2003.

Fan, H., Zhao, C. F., and Yang, Y. K.: A comprehensive analysis of the spatio-temporal variation of urban air pollution in China during 2014–2018, Atmos. Environ., 220, 117066, doi: 10.1016/j.atmosenv.2019.117066, 2020.

Gong, Y. W., Chen, Z. M., and Li, H.: The oxidation regime and SOA composition in limonene ozonolysis: roles of different double bonds, radicals, and water, Atmos. Chem. Phys., 18, 15105–15123, doi: 10.5194/acp-18-15105-2018, 2018.

Hasson, A. S., Ho, A. W., Kuwata, K. T., and Paulson, S. E.: Production of stabilized Criegee intermediates and peroxides in the gas phase ozonolysis of alkenes: 2. Asymmetric and biogenic alkenes, J. Geophys. Res., 106, 34143–34153, doi: 10.1029/2001JD000598, 2001.

Jonsson, A. M., Hallquist, M., and Ljungström, E.: Influence of OH scavenger on the water effect on secondary organic aerosol formation from ozonolysis of limonene, 3-carene, and α-pinene, Environ. Sci. Technol., 42, 5938–5944, doi: 10.1021/es702508y, 2008.

Keywood, M. D., Kroll, J. H., Varutbangkul, V., Bahreini, R., Flagan, R. C., and Seinfeld, J. H.: Secondary organic aerosol formation from cyclohexene ozonolysis: Effect of OH scavenger and the role of radical chemistry, Environ. Sci. Technol., 38, 3343–3350, doi: 10.1021/es049725j, 2004.

Khan, M. A. H., Percival, C. J., Caravan, R. L., Taatjes, C. A., and Shallcross, D. E.: Criegee intermediates and their impacts on the troposphere, Environ. Sci.: Processes Impacts, 20, 437–453, doi: 10.1039/C7EM00585G, 2018.

Kumar, M., Busch, D. H., Subramaniam, B., and Thompson, W. H.: Role of tunable acid catalysis in decomposition of hydroxyalkyl hydroperoxides and mechanistic implications for tropospheric chemistry, J. Phys. Chem. A, 118, 9701–9711, doi: 10.1021/jp505100x, 2014.

Lawrence, A. J. and Khan, T.: Indoor air quality assessment as related to household conditions in rural houses during winter season, Environ. Contam., 28, 221–244, doi: 10.1007/978-981-10-7332-8_11, 2017.

Lee, S. and Kamens, R. M.: Particle nucleation from the reaction of α-pinene and O_3, Atmos. Environ., 39, 6822–6832, doi: 10.1016/j.atmosenv.2005.07.062, 2005.

Lin, J. J. M. and Chao, W.: Structure-dependent reactivity of Criegee intermediates studied with spectroscopic methods, Chem. Soc. Rev., 46, 7483–7497, doi: 10.1039/C7CS00336F, 2017.

Paralovo, S. L., Barbosa, C. G. G., Carneiro, I. P. S., Kurzlop, P., Borillo, G. C., Schiochet, M. F. C., Godoi, A. F. L., Yamamoto, C. I., Souza, R. A. F., Andreli, R. V., Ribeiro. I. O., Manzi, A. O., Kourtchev, I., Bustillos, J. O. V., Martin, S. T., and Godoi, R. H. M.: Observations of particulate matter, NO_2, SO_2, O_3, H_2S and selected VOCs at a semi-urban environment in the Amazon region, Sci. Total Environ., 650, 996–1006, doi: 10.1016/j.scitotenv.2018.09.073, 2019.

Ravishankara, A. R.: Heterogeneous and multiphase chemistry in troposphere, Science, 276, 1058–1065, doi: 10.1126/science.276.5315.1058, 1997.

Sander, R.: Compilation of Henry's law constants (version 4.0) for water as solvent, Atmos. Chem. Phys., 15, 4399–4981, doi: 10.5194/acp-15-4399-2015, 2015.

Vereecken, L., Harder, H., and Novelli, A.: The reaction of Criegee intermediates with NO, RO_2, and SO_2, and their fate in the atmosphere, Phys. Chem. Chem. Phys., 14, 14682–14695, doi: 10.1039/c2cp42300f, 2012.

Wang, Y., Kim, H., and Paulson, S. E.: Hydrogen peroxide generation from α- and β-pinene and toluene secondary organic aerosols, Atmos. Environ., 45, 3149–3156, doi: 10.1016/j.atmosenv.2011.02.060, 2011.

Winterhalter, R., Neeb, P., Grossmann, D., Kolloff, A., Horie, O., and Moortgat, G.: Products and mechanism of the gas phase reaction of ozone with β-pinene, J. Atmos. Chem., 35, 165–197, doi: 10.1023/A:1006257800929, 2000.

Witkowski, B., Al-sharafi, M., and Gierczak, T.: Kinetics of limonene secondary organic aerosol oxidation in the aqueous phase, Environ. Sci. Technol., 52, 11583−11590, doi: 10.1021/acs.est.8b02516, 2018a.

Witkowski, B., Jurdana, S., and Gierczak, T.: Limononic acid oxidation by hydroxyl radicals and ozone in the aqueous phase, Environ. Sci. Technol., 52, 3402−3411, doi: 10.1021/acs.est.7b04867, 2018b.

Zhao, Q. L., Liu, F. Y., Wang, W. N., Li, C. Y., Lü, J., and Wang, W. L.: Reactions between hydroxyl-substituted alkylperoxy radicals and Criegee intermediates: correlations of the electronic characteristics of methyl substituents and the reactivity, Chem. Chem. Phys., 19, 15073, doi: 10.1039/c7cp00869d, 2017.

Zhao, R., Kenseth, C. M., Huang, Y. L., Dalleska, N. F., Kuang, X. M., Chen, J. R., Paulson, S. E., and Seinfeld, J. H.: Rapid aqueous-phase hydrolysis of ester hydroperoxides arising from Criegee intermediates and organic acids, J. Phys. Chem. A, 122, 5190−5201, doi: 10.1021/acs.jpca.8b02195, 2018.

Table S1. Wall loss fractions of SOA mass concentration at different relative humidity (RH).

RH	<0.5%	10%	20%	30%	40%	50%	60%	70%	80%	90%
Wall loss fraction (%)	7.21 ±0.72	6.57 ±0.77	6.88 ±0.82	7.02 ±0.93	7.65 ±0.95	8.21 ±0.88	11.29 ±0.90	13.04 ±1.21	15.67 ±1.16	17.10 ±1.45

Table S2. The amounts of SCIs (molecule cm^{-3}) under different concentrations of acetic acid (AA, molecule cm^{-3}) and different relative humidity (RH) in the first-generation oxidation.

AA \ RH	< 0.5%	10%	40%	60%	80%
0.00	2.66×10^{11}	1.84×10^{11}	1.45×10^{11}	1.38×10^{11}	1.21×10^{11}
5.90×10^{11}	1.85×10^{11}	1.66×10^{11}	1.38×10^{11}	1.27×10^{11}	1.19×10^{11}
1.18×10^{12}	1.16×10^{11}	1.03×10^{11}	8.30×10^{10}	9.81×10^{10}	9.01×10^{10}
2.36×10^{12}	6.94×10^{10}	6.29×10^{10}	6.10×10^{10}	6.41×10^{10}	6.04×10^{10}
3.54×10^{12}	5.17×10^{10}	4.16×10^{10}	2.56×10^{10}	5.24×10^{10}	4.35×10^{10}
4.72×10^{12}	2.80×10^{10}	1.65×10^{10}	1.19×10^{10}	2.74×10^{10}	2.90×10^{10}
5.90×10^{12}	1.21×10^{10}	4.57×10^{9}	3.82×10^{9}	1.39×10^{10}	1.93×10^{10}
7.08×10^{12}	2.95×10^{9}	2.26×10^{9}	-2.58×10^{9}	-2.22×10^{9}	7.73×10^{9}
8.27×10^{12}	1.23×10^{9}	1.83×10^{9}	-5.57×10^{9}	1.28×10^{9}	5.31×10^{9}
9.45×10^{12}	-1.97×10^{9}	1.89×10^{9}	-3.52×10^{9}	3.69×10^{9}	3.55×10^{9}
1.06×10^{13}	2.46×10^{9}	1.78×10^{9}	-5.45×10^{8}	3.25×10^{9}	5.09×10^{9}
1.18×10^{13}	-4.92×10^{8}	-9.65×10^{8}	-4.40×10^{8}	3.85×10^{9}	5.55×10^{9}

Note: The negative values appearing in the table were caused by the errors of measurements under high AA concentration.

Table S3. The amounts of SCIs (molecule cm^{-3}) under different concentrations of acetic acid (AA, molecule cm^{-3}) and different relative humidity (RH) in the second-generation oxidation.

AA \ RH	< 0.5%	10%	40%	60%	80%
0.00	2.21×10^{11}	1.60×10^{11}	1.29×10^{11}	1.65×10^{11}	2.41×10^{11}
5.90×10^{11}	1.45×10^{11}	1.38×10^{11}	1.13×10^{11}	1.12×10^{11}	1.77×10^{11}
1.18×10^{12}	1.01×10^{11}	1.02×10^{11}	8.79×10^{10}	9.10×10^{10}	1.09×10^{11}
2.36×10^{12}	6.05×10^{10}	5.33×10^{10}	6.16×10^{10}	6.13×10^{10}	7.84×10^{10}
3.54×10^{12}	5.49×10^{10}	4.50×10^{10}	5.54×10^{10}	5.47×10^{10}	4.68×10^{10}
4.72×10^{12}	4.75×10^{10}	4.49×10^{10}	4.61×10^{10}	4.79×10^{10}	2.86×10^{10}
5.90×10^{12}	3.84×10^{10}	2.98×10^{10}	3.79×10^{10}	2.55×10^{10}	1.49×10^{10}
7.08×10^{12}	1.97×10^{10}	1.91×10^{10}	2.88×10^{10}	2.24×10^{10}	1.21×10^{10}
8.27×10^{12}	1.21×10^{10}	9.06×10^{9}	1.94×10^{10}	2.16×10^{10}	1.03×10^{10}
9.45×10^{12}	9.84×10^{8}	6.89×10^{9}	1.38×10^{10}	1.85×10^{10}	1.01×10^{10}
1.06×10^{13}	-2.46×10^{8}	1.10×10^{9}	1.31×10^{10}	1.74×10^{10}	1.05×10^{10}
1.18×10^{13}	-2.46×10^{8}	9.78×10^{8}	1.24×10^{10}	1.77×10^{10}	1.03×10^{10}

Note: The negative values appearing in the table were caused by the errors of measurements under high AA concentration.

Table S4. The reactants concentrations (ppbv) in calculations of steady-state concentrations of SCIs in forest, urban area, and indoor area.

	Limonene	O_3	SO_2	NO_2
Forest	0.18	45	1[1]	2[2]
Urban area	0.15	45	10[3]	17[4]
Indoor area	2	20	10[5]	17[6]

[1] Boy et al., 2013; Paralovo et al., 2019

[2] Paralovo et al., 2019

[3] Fan et al., 2020

[4] Fan et al., 2020

[5] Lawrence and Khan, 2017

[6] Carslaw, 2007

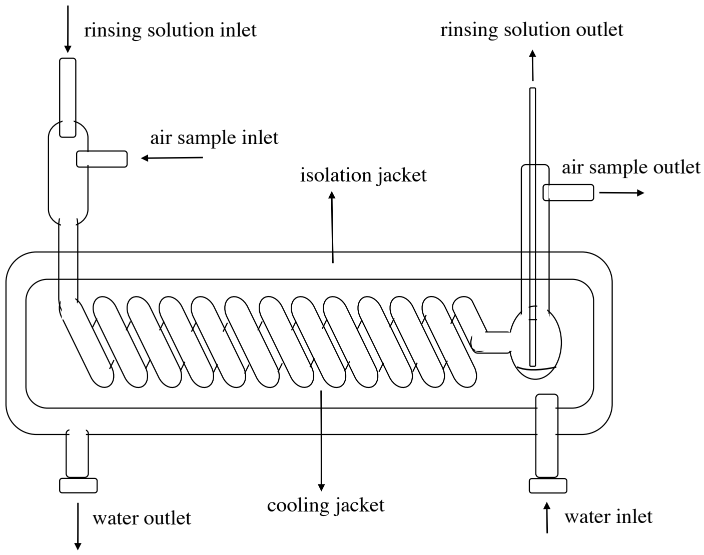

Figure S1. Diagram of the thermostatic coil collector.

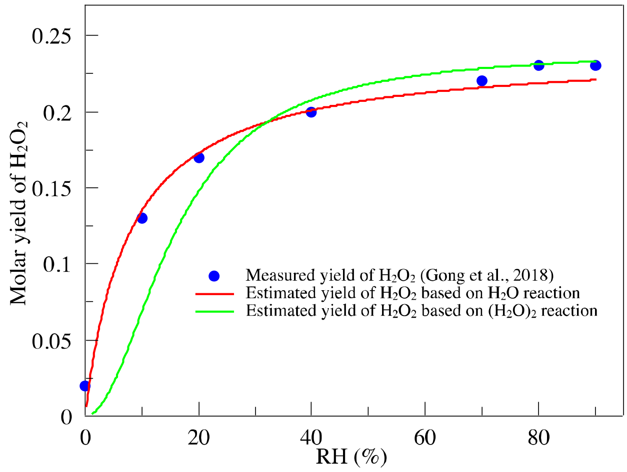

Figure S2. The dependence of the molar yield of hydrogen peroxide (H_2O_2) on relative humidity (RH). Blue dots: the measured yield of H_2O_2; Red line: the estimated yield of H_2O_2 based on SCI_I reaction with H_2O; Green line: the estimated yield of H_2O_2 based on SCI_I reaction with $(H_2O)_2$.

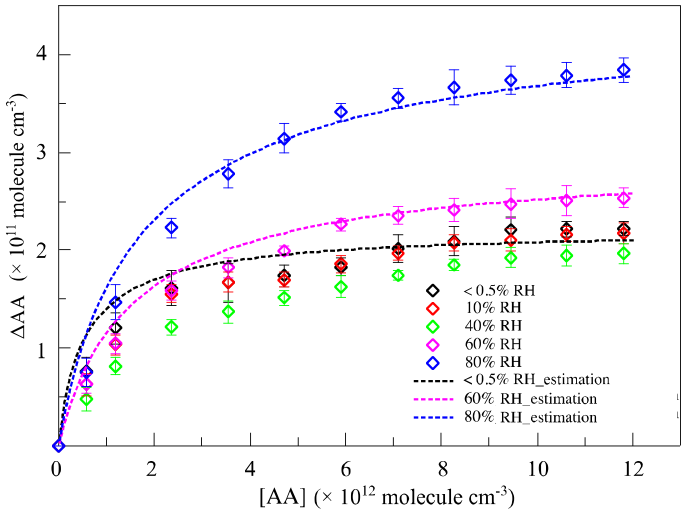

Figure S3. The variation of the consumption of acetic acid (ΔAA) with the concentration of acetic acid ([AA]) at different relative humidity (RH) in the second-generation oxidation. Scatters: measured ΔAA; Black line: estimated ΔAA at < 0.5% RH; Pink line: estimated ΔAA at 60% RH; Blue line: estimated ΔAA at 80% RH.

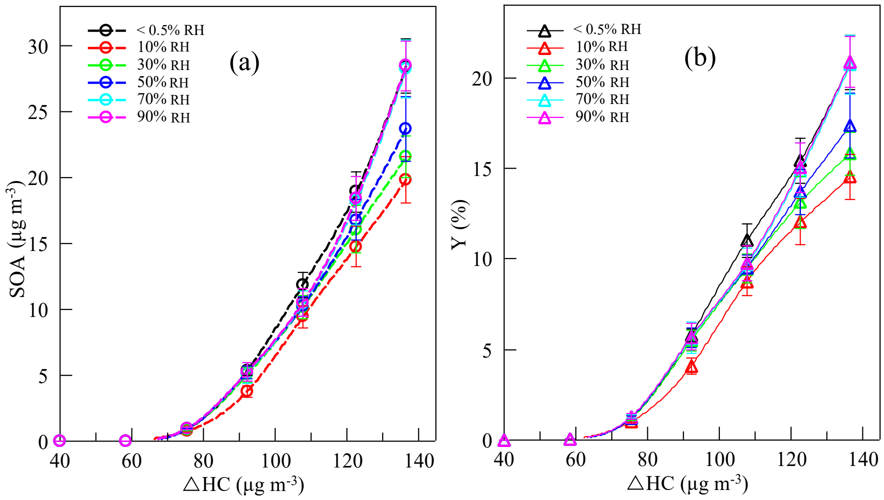

Figure S4. Growth curves of (a) SOA mass concentration (SOA) and (b) SOA yield (Y) versus limonene reacted (△HC) at different relative humidity (RH) in the first-generation oxidation.

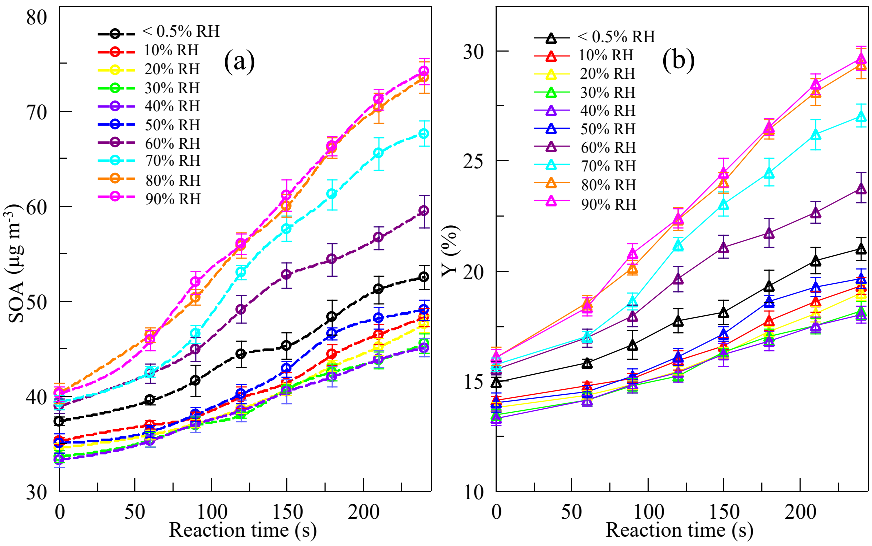

Figure S5. Growth curves of (a) SOA mass concentration (SOA) and (b) SOA yield (Y) versus reaction time at different relative humidity (RH) in the second-generation oxidation.

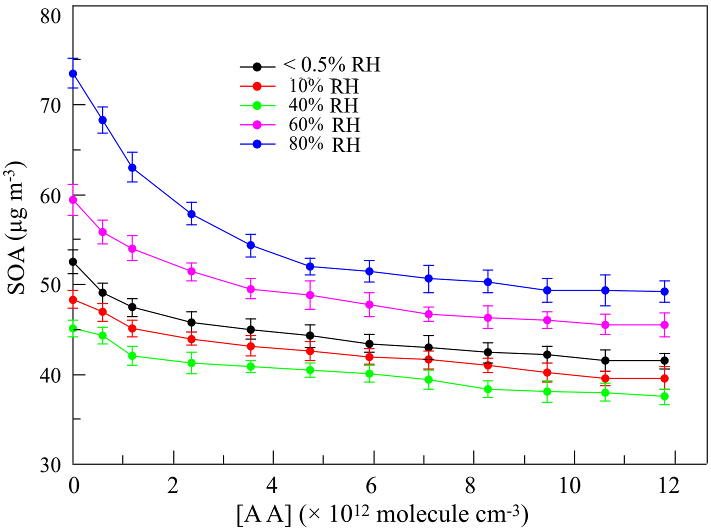

Figure S6. The variation of SOA mass concentration (SOA) with the concentration of acetic acid ([AA]) at different relative humidity (RH) in the second-generation oxidation.

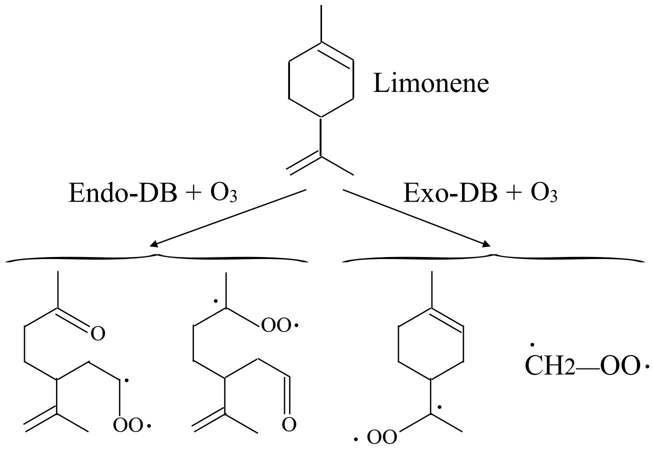

Figure S7. Structures of limonene-derived SCIs formed from endo-DB and exo-DB ozonolysis.

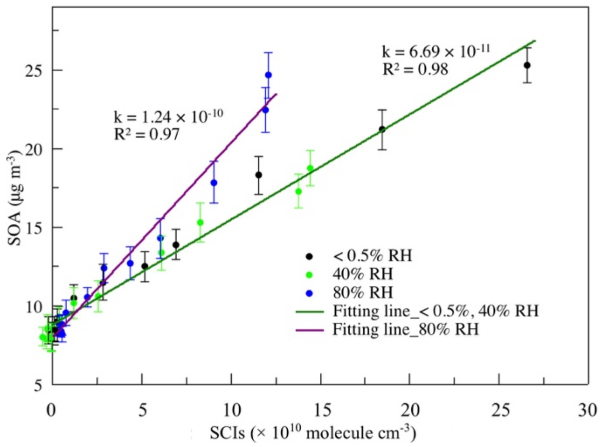

Figure S8. The dependence of SOA mass concentration on the amount of SCIs at different relative humidity (RH) in the first-generation oxidation with cyclohexane as OH scavenger.